All-Solid-State Batteries

Subjects: Energy & Fuels
Contributor: Gene Yang

All-solid-state batteries (SSBs) are one of the most fascinating next-generation energy storage systems that can provide improved energy density and safety for a wide range of applications from portable electronics to electric vehicles. The development of SSBs was accelerated by the discovery of new materials and the design of nanostructures. In particular, advances in the growth of thin-film battery materials facilitated the development of all solid-state thin-film batteries (SSTFBs)—expanding their applications to microelectronics such as flexible devices and implantable medical devices. However, critical challenges still remain, such as low ionic conductivity of solid electrolytes, interfacial instability and difficulty in controlling thin-film growth. In this review, we discuss the evolution of electrode and electrolyte materials for lithium-based batteries and their adoption in SSBs and SSTFBs. We highlight novel design strategies of bulk and thin-film materials to solve the issues in lithium-based batteries. We also focus on the important advances in thin-film electrodes, electrolytes and interfacial layers with the aim of providing insight into the future design of batteries. Furthermore, various thin-film fabrication techniques are also covered in this review.

Keywords: lithium-ion batteries ; solid electrolytes ; all solid-state batteries ; all solid-state thin-film batteries ; nanostructured thin films ; interfacial buffer layers ; thin-film techniques ; thin-film electrodes ; thin-film electrolytes

1. Introduction

Lithium-ion batteries (LIBs) are one of the great successes of electrochemical energy storage devices utilized in diverse applications such as portable electronics, hybrid automobiles and even large-scale electrical power storage systems [1][2][3][4]. Since the first market emergence of LIBs in the 1990s, the performance of LIBs has been remarkably improved to meet the increasing demand for new energy storage systems with high energy density, high power density, long cycle life and a wide range of operating temperatures [5][6]. Moreover, rechargeable batteries are rapidly expanding to drivetrains [7][8], as can be seen from the quadrupled global sales of plug-in light vehicles from 0.55 to 2.21 million cars annually from 2015 to 2019 [9]. Thus, developing revolutionary energy storage systems is a critical task in today's energy-dependent society.

LIBs are composed of a cathode and an anode separated by an electrolyte. During discharging, the lithium ions (Li^+) migrate through the electrolyte from the anode to the cathode and a discharging current flows through the external circuit, whereas the use of electrical energy pushes the electrons and Li^+ back to the anode during the charging process. Most of the commercial LIBs employ liquid electrolytes owing to their large electrochemical voltage windows, high ionic conductivities and great wettability with the internal components of LIBs [10]. Generally, the liquid electrolyte is a mixture of linear and cyclic carbonate-based organic solvents such as diethyl carbonate (DEC) [11], ethyl methyl carbonate (EMC) [11][12][13], dimethyl carbonate (DMC) [11][12], ethylene carbonate (EC) [12][13][14], propylene carbonate (PC) [11], and lithium salt such as lithium hexafluorophosphate ($LiPF_6$), lithium hexafluoroarsenate monohydrate ($LiAsF_6$), lithium perchlorate ($LiClO_4$) and lithium tetrafluoroborate ($LiBF_4$) [13][15][16]. However, these liquid electrolytes have severe drawbacks [17], including high flammability, narrow electrochemical stability windows, limited operating temperatures and irreversible decomposition. Due to their high flammability, organic liquid electrolytes are believed to be the main reason for fires and explosions in LIBs [18]. In addition, the formation of lithium dendrites with organic liquid electrolytes [19] leads to internal short circuits causing catastrophic failure of lithium-based batteries [20]. Therefore, developing alternative battery systems to prevent such issues of the liquid electrolytes as well as to provide high energy density and power is indispensable.

All-solid-state batteries (SSBs), which use non-volatile solid electrolytes, have emerged as an alternative battery system to replace the conventional LIBs with liquid electrolytes [21][22][23]. Not only are SSBs inherently safer owing to the lack of flammable organic components, SSBs also have a large electrochemical stability window, thus enabling a dramatic improvement in the energy density [24][25][26]. Furthermore, the SSBs have much higher power and energy characteristics compared with various batteries which are currently being developed as next-generation batteries [27][28]. The electrodes are required to have the following features in order to achieve high energy density: (i) high gravimetric capacity (in Ah/kg) and volumetric capacity (in Ah/L), i.e., a high number of electrons transferred per unit of reaction; (ii) high (cathode) and

low (anode) standard redox potential of the respective electrode redox reaction, leading to high cell voltage. Moreover, electrochemical reactions in rechargeable cells at both anode and cathode electrodes must be highly reversible to maintain the capacity for thousands of cycles. Recent studies, therefore, have focused on developing new electrode materials [29][30] or engineering electrode architectures [31][32] to increase the energy density of SSBs. Among various attractive candidate materials for electrodes, the selection of cathode materials depends on the battery type, i.e., Li^+ or Li-metal batteries. In the case of LIBs, air-stable lithium-based intercalation compounds should be used as a cathode due to the absence of lithium in the anode [33][34][35]. On the contrary, for Li-metal batteries, the cathode does not need to be lithiated before cell assembly owing to the use of metallic lithium as an anode [36]. Among a large number of materials proposed for the cathode in LIBs, transition metal oxides have been recognized as one of the most promising cathode materials [37][38][39]. For the anode, graphitic carbon allotropes were mostly used in LIBs, but the use of lithium metal can significantly increase the volumetric energy density by up to 70% with respect to graphite [40][41]. However, lithium metal electrodes encounter formidable challenges such as uncontrollable dendrite growth and high reactivity with solid electrolytes, which hampers the use of lithium metal electrodes [20]. Alternatively, recent studies of anode materials have focused on lithium transition metal oxides, vanadium oxides or lithium metal nitrides [42][43][44]. One of the key features of SSBs is replacing liquid electrolytes with solid electrolytes, which can dramatically enhance the safety of batteries. In order to replace the current organic liquid electrolytes, solid-state electrolytes need to possess high ionic conductivity, negligible electronic conductivity and good stability in contact with the anode and cathode electrodes [45][46]. Many different types of inorganic solid electrolytes—Na superionic conductor (NASICON) [47], perovskite [48], lithium phosphorous oxy-nitride (LiPON) [49][50][51], sulfide [52][53] and garnet [54][55][56]—are widely studied in SSBs.

With the development of SSBs, all-solid-state thin-film batteries (SSTFBs) have received significant attention in recent years [57][58][59] that can be used for low power microelectronic devices (e.g., implantable medical devices) and energy harvesting technologies [60]. Similar to conventional LIBs, SSTFBs consist of a cathode, an anode and an electrolyte. Owing to the difference in chemical potentials of lithium in the two electrodes, the transfer of Li^+ from the anode through the electrolyte into the cathode (discharge) delivers energy, whereas the reverse lithium transfer (charge) consumes energy. One unique feature of SSTFBs is the usage of nanostructured thin films and thus SSTFBs can significantly reduce the transport distance of charge carriers, enhancing the kinetics of lithium storage [61][62]. Furthermore, the overall performance of SSTFBs can be controlled by modulating the physical and chemical properties of thin films. In order to make SSTFBs, all the battery components need to be fabricated into multilayered thin films by suitable thin-film techniques.

While SSBs and SSTFBs have shown their potential as the next major advances beyond LIBs, their performances have not yet been reached the practical level mainly due to the limits of intrinsic material properties. Therefore, understanding and controlling the properties of electrode and electrolyte materials will provide insight into the enhancement of the next-generation battery performances.

2. Electrodes and Electrolytes for Lithium-Based Batteries

As described earlier, the alleviation of safety concerns by using solid electrolytes is the key feature of SSBs. Moreover, solid electrolytes exhibit a large electrochemical window (up to five volts), which can enable the utilization of high voltage cathode materials as well as lithium metal anode.

2.1. Electrodes

Selecting electrode materials for the next generation of batteries needs careful considerations with regards to safety, energy density, cost, cyclability, crustal abundance and recyclability. Electrode chemistries which rely on the mining of rare elements and the utilization of complex ceramic processing greatly diminish the sustainability of an electrode material [63]. In addition to the extraction and processing of raw materials, a holistic approach considering the electrode synthesis and device fabrication must be taken into the actual energy cost of battery fabrications.

2.2. Solid Electrolytes

The NASICON structure, standing for Na^+ superionic conductors, was reported by Hangman et al. in 1968 [64]. It has a rhombohedral structure (space group R-3c) made of the framework of octahedra (MO_6, M = divalent to pentavalent transition metal ions) and tetrahedra (XO_4, X = P, Si, As). Two MO_6 octahedra and three PO_4 tetrahedra share oxygen atoms, which are assembled to form a 3D network structure. This structure provides a 3D interconnected conduction pathway for mobile ions, most commonly Na^+ or Li^+ [65]. The NASICON structure can have a wide range of compositional varieties, leading to varied ionic conductivities. The most promising NASICON-type Li^+ conductors are $LiTi_2(PO_4)_3$ and $LiGe_2(PO_4)_3$ with Al substitutions. Arbi et al. [66] reported the synthesis of $Li_{1+x}Al_xTi_{2-x}(PO_4)_3$ (LATP) and $Li_{1+x}Al_xGe_{2-x}(PO_4)_3$ (LAGP) conductors ($0 \le x \le 0.5$) giving conductivities of 3.4×10^{-3} S/cm (LATP, x = 0.2) and 10^{-4}

S/cm (LAGP, x = 0.2) at room temperature. By enhancing the crystallization of LAGP, Thokchom et al. [67] reported a conductivity of 4.22 × 10^{-3} S/cm at room temperature. Although its high ionic conductivity is attractive, the instability of LATP in contact with Li metal due to the reduction of Ti^{4+} requires an additional protective layer. Furthermore, expensive precursors to synthesize LAGP would require the substitution of Ge. As prototype cells, LAGP was used for a Li protection membrane for aqueous Li–air batteries [68][69].

By the 1980s, a considerable amount of work had been done on inorganic solid lithium superionic conductors, $Li_{4\pm x}Si_{1-x}X_xO_4$ (X = P, Al or Ge, LISICON) [70]. LISICON is based on the γ-Li_3PO_4 structure that is expected to diffuse Li^+ through the vacancy mechanism in its pure state. The ionic conductivity of $Li_{14}ZnGe_4O_{16}$ was limited to 10^{-7} S/cm at room temperature and had reactivity with Li anode or atmospheric CO_2 [71]. Kuwano and West in 1980 reported much higher ionic conductivity for Li_4GeO_4–Li_3VO_4 systems with a total ionic conductivity of 4 × 10^{-5} S/cm at 18 °C with the addition of an interstitial diffusion mechanism [72]. The introduction of V^{5+} (e.g., $Li_{3+x}Ge_xV_{1-x}O_4$) contributed to stabilizing the structure in the presence of CO_2 in air. It is also reported that the Li_4SiO_4–Li_3PO_4 solid solution presented the ionic conductivity 10^{-6} S/cm at room temperature and had better stability against Li due to the absence of transition metal ions. While maintaining the chemical stability in Li_4Si/GeO_4–Li_3PO_4 solid solution, the ionic conductivity could be further improved to ~10^{-5} S/cm by substituting O with Cl, enlarging the four oxygen bottleneck size and lowering the diffusion barriers [73]. The most significant conductivity improvement of the LISICON structure was achieved with O replacement with larger and better polarizing ions, S, to form thio-LISICON. For example, the Li_2S–GeS2–P_2S_5 system ($Li_{3.25}Ge_{0.25}P_{0.75}S_4$, called LGPS) reached a high ionic conductivity of 2.2 × 10^{-3} S/cm at room temperature [74]. However, the high sensitivity to moisture in air and difficulties in the synthesis of sulfide electrolytes remain as challenges.

In 1992, Bates et al. [75] reported the synthesis of lithium phosphorus oxynitride (LiPON, $Li_{3.3}PO_{3.9}N_{0.17}$) by RF-magnetron sputtering of Li_3PO_4, which showed conductivity of 2 × 10^{-6} S/cm at 25 °C. Different from other electrolytes, LiPON has an amorphous structure, and its ionic conductivity is significantly affected by the amount of nitrogen [76][77][78]. Another route to improve the ionic conductivity of LiPON is to increase the Li concentration, as can be seen by the conductivity increase to 6.4 × 10^{-6} S/cm at 25 °C when LiPON was deposited with Li_2O in addition to Li_3PO_4. Because of its easy deposition in thin films, LiPON can present a low resistance in the form of a thin film. Thus, LiPON is commonly used as the electrolyte for thin-film microbatteries (1–10 mAh) that can be used for smart cards, wearable devices, MEMS or implantable medical devices [79][80]. The deposition of LiPON and prototype battery performance will be discussed in detail later.

Among perovskite-type solid electrolyte materials, $Li_xLa_{2/3-1/3x}TiO_3$ (LLTO) exhibited very high bulk ionic conductivity. The LLTO is composed of the ideal structure cubic phase α-LLTO with Pm3 m symmetry and tetragonal phase β-LLTO with a P4/mmm space group. In 1993, Inaguma et al. [81] showed the improved ionic conductivity of $Li_{0.34}La_{0.51}TiO_{2.94}$ compared to LISICON. The bulk and grain boundary activation energies of the cubic perovskite structure were reported to be E_b = 0.40 eV and E_{gb} = 0.42 eV, respectively. Importantly, the bulk ionic conductivity was reported to be 1 × 10^{-3} S/cm at room temperature, but the total ionic conductivity was 2 × 10^{-5} S/cm due to the high grain boundary resistance. Alonso et al. [82] identified the position of Li^+ in $Li_{0.5}La_{0.5}TiO_3$ using the neutron powder diffraction and suggested the Li^+ conduction pathway in LLTO. Jay et al. [83] proposed an additional diffusion pathway in the c-direction via a computational study that aligned more directly with experimental data. Lu et al. [84] synthesized $Li_{2x-y}Sr_{1-x-y}La_yTiO_3$ to enhance the Li^+ diffusion by increasing A site. With the composition of $Li_{15/56}Sr_{1/16}La_{15/28}TiO_3$ a total conductivity of 4.84 × 10^{-4} S/cm was achieved with an activation energy of just 0.29 eV.

Although its high bulk ionic conductivity is attractive, LLTO suffers from high grain boundary resistance and reactivity with Li metal. LLTO variants showed distinct discoloration when in contact with Li metal, and the Li intercalation at 1.7 V vs. Li/Li^+ into LLTO was observed, limiting their use with low potential anode materials [85][86][87]. To resolve the instability issue of LLTO with Li, Ti^{4+} was substituted with Ge^{4+} [88] or Zr^{4+} and Ta^{5+} [89] extending the cathodic stability limit of perovskites to 0–1 V vs. Li/Li^+.

3. Interfacial Phenomena between Solid-State Electrolytes and Electrodes

As described in previous sections, substantial effort has been devoted to developing high energy and power density electrodes, solid-state electrolytes with high ionic conductivity, good chemical stability and large electrochemical stability windows. However, the performance enhancement of batteries can be insignificant despite the dramatically enhanced performance of an individual component, i.e., electrodes or electrolytes. More importantly, the power density and cycle life of SSBs still have not met the requirements for practical applications. Such poor performances are mainly attributed to the large interfacial resistance between solid electrolytes and electrodes [90][91][92][93] that originates from the mechanical force

development or chemical composition changes. These configurational and chemical changes driven by electrochemical reactions are summarized in Figure 1 [94][95]. We will discuss mechanical and chemical factors associated with the large interfacial resistance in the following section.

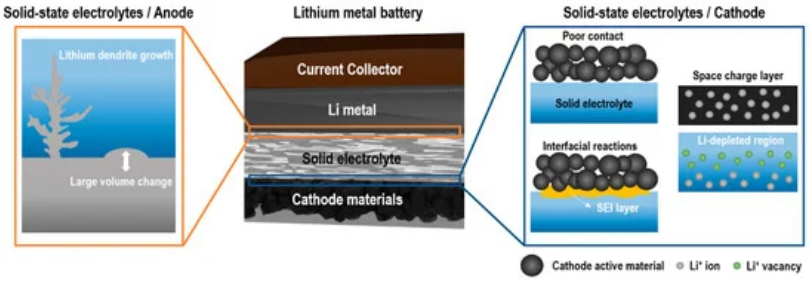

Figure 1. Schematic diagram of lithium metal battery and electrode/electrolyte interface issues.

Mechanically driven interfacial resistance between solid electrolytes and electrodes originates from poor contact between two rigid materials and the volume changes of electrodes during the charge–discharge process [96]. This poor contact eventually leads to the formation and propagation of cracks [97] as well as the delamination of interfaces [98][99]. Sulfide-based electrolytes possess good mechanical ductility, thus can maintain good contact with electrodes without the degradation of the interfacial contact resistance [100]. In contrast, oxide-based electrolytes suffer from the poor adhesion of interfaces with electrodes as most ceramics are vulnerable to cracking due to the low ductility [101][102]. The insufficient mechanical contact results in the delamination or “dead” area induced by isolated electrode contact points from solid electrolytes. Due to the lack of conduction paths, neither electrons nor Li^+ can be transferred across the dead areas, which in turn leads to the growth of interfacial resistance and capacity fading [103]. Furthermore, the large volume changes of electrode materials during repeated charge–discharge processes could also lead to the loss of effective contact between electrodes and solid electrolytes [104]. Zhang et al. [98] first demonstrated changes in the pressure and height of LCO/$Li_{10}GeP_2S_{12}$/In and LCO/$Li_{10}GeP_2S_{12}$/LTO under galvanostatic cycling where the volume expansions of LCO, LTO and In were found to be 2%, 0.2% and 105.6%, respectively. Due to the significant volume change of In, the LCO/$Li_{10}GeP_2S_{12}$/In cell showed severe capacity fading. Similarly, Koerver et al. [100] detected the increased interfacial resistance and capacity fading caused by the contact loss at the NCM-811/β-Li_3PS_4 interface.

The occurrence of the interfacial resistance by the formation of interlayers is a well-known phenomenon in SSBs. One of the main reasons for the interfacial resistance is the formation of space charge regions (SCRs). SCRs originate from the depletion of lithium near the interface between the cathode and the electrolyte in SSBs due to the high potential gradient [105]. The potential difference at this interface causes Li^+ to move toward a higher potential region, causing lithium depletion and increasing the ionic resistance at the interface. Sulfide-based electrolytes exhibit a weaker interaction with Li^+ and lower chemical potential of Li^+ compared with those of oxide cathodes, such as LCO. Thus, the Li^+ in sulfide-based electrolytes will migrate into the oxide cathode easily, resulting in the redistribution of Li^+ at the interface which forms lithium depletion layers, SCRs [106]. Unlike sulfide-based electrolytes, the influence of SCRs is smaller in oxide-based electrolytes because the chemical potential of Li^+ in oxide electrolytes is comparable with that in the cathode [107]. At the interface between LCO and $Li_{1+x+y}Al_yTi_{2-y}Si_xP_{3-x}O_{12}$, the thickness of SCRs in the sulfide-based electrolyte was thicker than 1 μm determined by measuring the electric potential profile with transmission electron microscopy (TEM) [108]. A similar SCR thickness was also reported in $LiCoPO_4$/$Li_{1+x}Al_xTi_{2-x}(PO_4)_3$ using Kelvin probe force microscopy (KPFM) [109]. On the contrary, the thickness estimated from the resistance (~10 Ω cm^2) at the LiPON/LCO interface was found to be in the range of nanometers [110]. De Klerk et al. [111] also estimated the nanometer-thick SCRs based on the interfacial resistance (17 Ω cm^2) between the solid electrolytes, i.e., garnet and NASICON (LLZO and $Li_{1.2}Al_{0.2}Ti_{1.8}(PO_4)_3$) and the cathode (LCO) or anode (graphite).

Interfacial chemical reactions derived from the interdiffusion between electrodes and solid electrolytes can also contribute to high interfacial resistance [112]. These interfacial reactions can form an interphase layer known as SEI at the electrode/electrolyte interface by consuming Li^+ and electrons from electrodes. The electrical properties of the SEI layer play a role in determining how the reaction between electrolytes and electrodes continues [113][114][115]. This SEI layer continues to grow until it blocks the Li^+ transport over the electrolyte/electrode. Park et al. [116] showed that an approximately 50-nm-thick layer forms in the vicinity of the LCO/Garnet interface due to the mutual diffusion of Co, La and Zr which leads to capacity fading. In addition, Wenzel et al. [117] also revealed that Li_3P, Li_2S and Li–Ge alloys form a SEI layer upon the reaction of $Li_{10}GeP_2S_{12}$ solid electrolyte with Li metal by in situ X-ray photoemission spectroscopy.

As a general strategy to resolve the aforementioned issue at the electrode/electrolyte interface, nanometer-thick interfacial buffer layers have been grown to enhance the performance of the SSBs [118][119]. Consequently, it is critical to employ thin-film growth techniques that can provide high purity and desired crystallinity of target materials in SSBs' assembly processes. Furthermore, the growth of thin films is a key success factor in building SSTFBs that have dramatically reduced charge-transfer resistance throughout the device. Therefore, understanding the precise control of thin-film growth and determining the impact of thin films on battery performances are requisite.

4. Electrodes and Electrolytes for SSTFBs

To meet the increasing demand for portable (micro-)electronic applications in today's information-rich and mobile society, developing rechargeable battery systems with high energy density and reduced dimensions is crucial. For such battery systems, SSTFBs are one of the most attractive battery systems owing to their shape, versatility, flexibility and lightness [120][121][122]. Since being first introduced in 1983 [123], SSTFBs have been continuously studied over the past four decades [122][124][125][126][127][128][129]. In recent years, considerable progress has been made in the development of SSTFBs along with advances in thin-film technologies [130][131]. SSTFBs provide unique advantages such as outstanding cycle life and safety compared to conventional LIBs [132][133]. Moreover, SSTFBs enable the miniaturization of LIBs required for applications, including implantable medical devices, wireless microsensors, microelectromechanical system devices and flexible electronics [134][135].

SSTFBs are composed of multiple micron-sized electrochemical cells consisting of a cathode and an anode electrode separated by an electrolyte. A thin-film electrochemical cell is generally fabricated on a solid substrate like glass, ceramic or even polymer. The first layer is usually a current collector, then followed by the electrode, electrolyte, electrode and another layer of a current collector. Generally, the thickness of thin films in SSTFBs is in the range of nanometers to microns. Such thin layers can significantly enhance the charge transfer kinetics [136] which prevents the local overcharging and discharging issue reported in conventional battery systems [136]. In addition, SSTFBs use dense thin films without a polymeric binder and thus can be used as an ideal system for the fundamental understanding of energy storage mechanisms. Furthermore, SSTFBs have higher volumetric and gravimetric power density (Figure 2) compared to other battery systems [137]. The use of thin-film electrochemical cells is therefore a promising and practical strategy to fully utilize the advantage of lithium-based batteries for diverse applications.

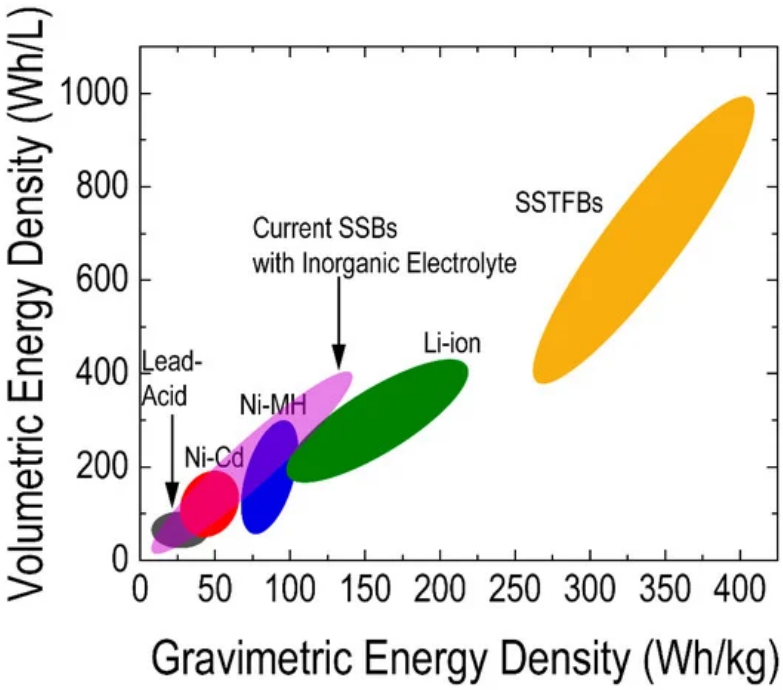

Figure 2. Comparison of the volumetric and gravimetric energy density of solid-state thin-film batteries (SSTFBs) with other batteries [138][139][140]

5. Conclusions

Replacing liquid electrolytes with solid counterparts allows SSBs to exhibit excellent safety, electrochemical stability and high energy density. Despite these advantages, further enhancement of the current SSBs is required to be used in practical applications. Improving the material properties of electrodes and electrolytes may accelerate the development of the next-generation energy storage systems. This review discussed key advances in battery materials and possible

solutions to solve their issues. Surface modification, doping and nanostructuring have been successfully used to improve the electrode performance. For the solid electrolyte, many efforts have been devoted to improving the ionic conductivity by doping or altering the crystal structures. Indeed, several studies have improved the thermal and chemical stability of the solid electrolytes by replacing sensitive elements, such as transition metals. While we mainly focused on oxide-based solid electrolytes, LiRAP and sulfide-based solid electrolytes are becoming increasingly attractive owing to their outstanding ionic conductivity. However, the highly air sensitive nature of these electrolytes remains a substantial obstacle.

Over the last few decades, the development of oxide thin films has led to many technological breakthroughs for energy and electronic devices. In particular, 2D planar heterostructures have been prevailingly investigated as they lead not only to improved functionalities but even to the occurrence of novel properties that do not belong to the bulk [141][142]. For instance, the discovery of the formation of a conducting interface between two insulators [142], STO and $LaAlO_3$ (LAO), brought the breakthrough in the field of oxide electronics while also becoming the pole of attraction and inspiration for numerous studies [143][144]. Recently, a couple of attempts have been made to utilize heterostructure thin films in lithium-based batteries [145][146][147]. In addition, developing new forms of materials with tailored properties could bring technological breakthroughs in the next-generation energy storage systems. For example, 3D nanostructures can offer an extremely large number of interfaces and surface area, which are beneficial for enhancing the electrochemical performance and ion transport in materials [148][149]. To date, a few studies have been investigated the influence of 3D nanostructures on the performance of lithium-based batteries [150][151]. Exploring new forms of materials will bring new opportunities to develop high-performance electrodes and electrolytes for SSBs and SSTFBs

References

1. Zhang, J.; Zhang, L.; Sun, F.; Wang, Z. An overview on thermal safety issues of lithium-ion batteries for electric vehicle application. IEEE Access 2018, 6, 23848–23863.
2. Dubarry, M.; Devie, A. Battery durability and reliability under electric utility grid operations: Representative usage aging and calendar aging. J. Energy Storage 2018, 18, 185–195.
3. Lopez, J.; Gonzalez, M.; Viera, J.C.; Blanco, C. Fast-charge in lithium-ion batteries for portable applications. In Procee dings of the INTELEC 2004. 26th Annual International Telecommunications Energy Conference, Chicago, IL, USA, 19–23 September 2004.
4. Karden, E.; Ploumen, S.; Fricke, B.; Miller, T.; Snyder, K. Energy storage devices for future hybrid electric vehicles. J. P ower Sources 2007, 168, 2–11.
5. Nishi, Y. Lithium ion secondary batteries: Past 10 years and the future. J. Power Sources 2001, 100, 101–106.
6. Ge, S.; Leng, Y.; Liu, T.; Longchamps, R.S.; Yang, X.G.; Gao, Y.; Wang, D.; Wang, D.; Wang, C.Y. A new approach to b oth high safety and high performance of lithium-ion batteries. Sci. Adv. 2020, 6, eaay7633.
7. Schmidt, M.; Neuschütz, M. Lithium-ion batteries key component electrolyte. ATZ Worldw. 2011, 6, 10–15.
8. Kwade, A.; Haselrieder, W.; Leithoff, R.; Modlinger, A.; Dietrich, F.; Droeder, K. Current status and challenges for autom otive battery production technologies. Nat. Energy 2018, 3, 290–300.
9. Plug-in Electric Light Vehicle Sales Worldwide 2015–2019. Available online: https://www.statista.com/statistics/665774/global-sales-of-plug-in-light-vehicles/#:~:text =In%202019%2C%20around%202.2%20million,(PEV)%20were%20sold%20worldwide (accessed on 11 June 2020).
10. Peljo, P.; Girault, H.H. Electrochemical potential window of battery electrolytes: The HOMO-LUMO misconception. Ener gy Environ. Sci. 2018, 11, 2306–2309.
11. Eshetu, G.G.; Grugeon, S.; Laruelle, S.; Boyanov, S.; Lecocq, A.; Bertrand, J.P.; Marlair, G. In-depth safety-focused an alysis of solvents used in electrolytes for large scale lithium ion batteries. Phys. Chem. Chem. Phys. 2013, 15, 9145–9155.
12. Fu, Y.; Lu, S.; Shi, L.; Cheng, X.; Zhang, H. Combustion characteristics of electrolyte pool fires for lithium ion batteries. J. Electrochem. Soc. 2016, 163, A2022–A2028.
13. Fan, H.; Qi, L.; Yoshio, M.; Wang, H. Hexafluorophosphate intercalation into graphite electrode from ethylene carbonat e/ethylmethyl carbonate. Solid State Ion. 2017, 304, 107–112.
14. Ding, W.; Lei, X.; Ouyang, C. Coordination of lithium ion with ethylene carbonate electrolyte solvent: A computational st udy. Int. J. Quantum Chem. 2016, 116, 97–102.

15. Younesi, R.; Veith, G.M.; Johansson, P.; Edström, K.; Vegge, T. Lithium salts for advanced lithium batteries: Li-metal, Li-O2, and Li-S. Energy Environ. Sci. 2015, 8, 1905–1922.

16. Liu, L.; Gu, S.; Wang, S.; Zhang, X.; Chen, S. A LiPO2F2/LiPF6 dual-salt electrolyte enabled stable cycling performance of nickel-rich lithium ion batteries. RSC Adv. 2020, 10, 1704–1710.

17. Miller, T.F.; Wang, Z.G.; Coates, G.W.; Balsara, N.P. Designing polymer electrolytes for safe and high capacity rechargeable lithium batteries. Acc. Chem. Res. 2017, 50, 590–593.

18. Arbizzani, C.; Gabrielli, G.; Mastragostino, M. Thermal stability and flammability of electrolytes for lithium-ion batteries. J. Power Sources 2011, 196, 4801–4805.

19. Takehara, Z.I. Future prospects of the lithium metal anode. J. Power Sources 1997, 68, 82–86.

20. Takeda, Y.; Yamamoto, O.; Imanishi, N. Lithium dendrite formation on a lithium metal anode from liquid, polymer and solid electrolytes. Electrochemistry 2016, 84, 210–218.

21. Xu, R.C.; Wang, X.L.; Zhang, S.Z.; Xia, Y.; Xia, X.H.; Wu, J.B.; Tu, J.P. Rational coating of Li7P3S11 solid electrolyte on MoS2 electrode for all-solid-state lithium ion batteries. J. Power Sources 2018, 374, 107–112.

22. Yang, J.; Wang, X.; Zhang, G.; Ma, A.; Chen, W.; Shao, L.; Shen, C.; Xie, K. High-performance solid composite polymer electrolyte for all solid-state lithium battery through facile microstructure regulation. Front. Chem. 2019, 7, 338.

23. Xu, H.; Chien, P.H.; Shi, J.; Li, Y.; Wu, N.; Liu, Y.; Hu, Y.Y.; Goodenough, J.B. High-performance all-solid-state batteries enabled by salt bonding to perovskite in poly (ethylene oxide). Proc. Natl. Acad. Sci. USA 2019, 116, 18815–18821.

24. Chen, J.; Huang, X.; Zhu, Y.; Jiang, P. Cellulose nanofiber supported 3D interconnected BN nanosheets for epoxy nanocomposites with ultrahigh thermal management capability. Adv. Funct. Mater. 2017, 27, 1604754.

25. Hou, H.; Xu, Q.; Pang, Y.; Li, L.; Wang, J.; Zhang, C.; Sun, C. Efficient storing energy harvested by triboelectric nanogenerators using a safe and durable all-solid-state sodium-ion battery. Adv. Sci. 2017, 4, 1700072.

26. Simonetti, E.; Carewska, M.; Maresca, G.; De Francesco, M.; Appetecchi, G.B. Highly conductive, ionic liquid-based polymer electrolytes. J. Electrochem. Soc. 2016, 164, A6213–A6219.

27. Kato, Y.; Hori, S.; Saito, T.; Suzuki, K.; Hirayama, M.; Mitsui, A.; Yonemura, M.; Iba, H.; Kanno, R. High-power all-solid-state batteries using sulfide superionic conductors. Nat. Energy 2016, 1, 16030.

28. Gür, T.M. Review of electrical energy storage technologies, materials and systems: Challenges and prospects for large-scale grid storage. Energy Environ. Sci. 2018, 11, 2696–2767.

29. Wu, X.; Yao, S. Flexible electrode materials based on WO3 nanotube bundles for high performance energy storage devices. Nano Energy 2017, 42, 143–150.

30. Wu, F.; Yushin, G. Conversion cathodes for rechargeable lithium and lithium-ion batteries. Energy Environ. Sci. 2017, 10, 435–459.

31. Taberna, P.L.; Mitra, S.; Poizot, P.; Simon, P.; Tarascon, J.M. High rate capabilities Fe3O4-based Cu nano-architectured electrodes for lithium-ion battery applications. Nat. Mater. 2006, 5, 567–573.

32. Liu, W.; Lin, D.; Pei, A.; Cui, Y. Stabilizing lithium metal anodes by uniform Li-ion flux distribution in nanochannel confinement. J. Am. Chem. Soc. 2016, 138, 15443–15450.

33. Armstrong, A.R.; Bruce, P.G. Synthesis of layered LiMnO2 as an electrode for rechargeable lithium batteries. Nature 1996, 381, 499–500.

34. Zhao, J.; Zhang, W.; Huq, A.; Misture, S.T.; Zhang, B.; Guo, S.; Wu, L.; Zhu, Y.; Chen, Z.; Amine, K.; et al. In Situ probing and synthetic control of cationic ordering in Ni-rich layered oxide cathodes. Adv. Energy Mater. 2017, 7, 1601266.

35. Zheng, J.; Liu, T.; Hu, Z.; Wei, Y.; Song, X.; Ren, Y.; Wang, W.; Rao, M.; Lin, Y.; Chen, Z.; et al. Tuning of thermal stability in layered Li(NixMnyCoz)O2. J. Am. Chem. Soc. 2016, 138, 13326−13334.

36. Zhao, J.; Zhou, G.; Yan, K.; Xie, J.; Li, Y.; Liao, L.; Jin, Y.; Liu, K.; Hsu, P.C.; Wang, J.; et al. Air-stable and freestanding lithium alloy/graphene foil as an alternative to lithium metal anodes. Nat. Nanotechnol. 2017, 12, 993–999.

37. Zheng, M.; Tang, H.; Li, L.; Hu, Q.; Zhang, L.; Xue, H.; Pang, H. Hierarchically nanostructured transition metal oxides for lithium-ion batteries. Adv. Sci. 2018, 5, 1700592.

38. Liu, H.; Bugnet, M.; Tessaro, M.Z.; Harris, K.J.; Dunham, M.J.R.; Jiang, M.; Goward, G.R.; Botton, G.A. Spatially resolved surface valence gradient and structural transformation of lithium transition metal oxides in lithium-ion batteries. Phys. Chem. Chem. Phys. 2016, 18, 29064–29075.

39. Shukla, A.K.; Ramasse, Q.M.; Ophus, C.; Kepaptsoglou, D.M.; Hage, F.S.; Gammer, C.; Bowling, C.; Gallegos, P.A.H.; Venkatachalam, S. Effect of composition on the structure of lithium- and manganese-rich transition metal oxides. Energy Environ. Sci. 2018, 11, 830–840.

40. Chan, C.K.; Zhang, X.F.; Cui, Y. High capacity Li ion battery anodes using Ge nanowires. Nano Lett. 2008, 8, 307–309.

41. Meduri, P.; Pendyala, C.; Kumar, V.; Sumanasekera, G.U.; Sunkara, M.K. Hybrid tin oxide nanowires as stable and high capacity anodes for Li-ion batteries. Nano Lett. 2009, 9, 612–616.

42. Guyomard, D.; Sigala, C.; de Gal La Salle, A.; Piffard, Y. New amorphous oxides as high capacity negative electrodes f or lithium batteries: The LixMVO4 (M = Ni, Co, Cd, Zn; 1 < x ≤ 8) series. J. Power Sources 1997, 68, 692–697.

43. Piffard, Y.; Leroux, F.; Guyomard, D.; Mansot, J.L.; Tournoux, M. The amorphous oxides MnV2O6+δ (0 < δ < 1) as high capacity negative electrode materials for lithium batteries. J. Power Sources 1997, 68, 698–703.

44. Shodai, T.; Okada, S.; Tobishima, S.; Yamaki, J. Anode performance of a new layered nitride Li3−xCoxN (x = 0.2–0.6). J. Power Sources 1997, 68, 515–518.

45. Goodenough, J.B.; Kim, Y. Challenges for rechargeable Li batteries. Chem. Mater. 2010, 22, 587–603.

46. Xu, R.; Han, F.; Ji, X.; Fan, X.; Tu, J.; Wang, C. Interface engineering of sulfide electrolytes for all-solid-state lithium bat teries. Nano Energy 2018, 53, 958–966.

47. Wang, G.X.; Bradhurst, D.H.; Dou, S.X.; Liu, H.K. LiTi2(PO4)3 with NASICON-type structure as lithium-storage material s. J. Power Sources 2003, 124, 231–236.

48. Li, Y.; Xu, H.; Chien, P.H.; Wu, N.; Xin, S.; Xue, L.; Park, K.; Hu, Y.Y.; Goodenough, J.B. A perovskite electrolyte that is stable in moist air for lithium-ion batteries. Angew. Chem. Int. Ed. 2018, 57, 8587–8591.

49. Al-Qawasmeh, A.; Holzwarth, N.A.W. Li14P2O3N6 and Li7PN4: Computational study of two nitrogen rich crystalline LiP ON electrolyte materials. J. Power Sources 2017, 364, 410–419.

50. Asano, T.; Sakai, A.; Ouchi, S.; Sakaida, M.; Miyazaki, A.; Hasegawa, S. Solid halide electrolytes with high lithium-ion c onductivity for application in 4 V class bulk-type all-solid-state batteries. Adv. Mater. 2018, 30, 1803075.

51. Maekawa, H.; Matsuo, M.; Takamura, H.; Ando, M.; Noda, Y.; Karahashi, T.; Orimo, S.I. Halide-stabilized LiBH4, a room -temperature lithium fast-ion conductor. J. Am. Chem. Soc. 2009, 131, 894–895.

52. Seino, Y.; Ota, T.; Takada, K.; Hayashi, A.; Tatsumisago, M. A sulphide lithium super ion conductor is superior to liquid i on conductors for use in rechargeable batteries. Energy Environ. Sci. 2014, 7, 627–631.

53. Kamaya, N.; Homma, K.; Yamakawa, Y.; Hirayama, M.; Kanno, R.; Yonemura, M.; Kamiyama, T.; Kato, Y.; Hama, S.; K awamoto, K.; et al. A lithium superionic conductor. Nat. Mater. 2011, 10, 682–686.

54. Fu, K.K.; Gong, Y.; Xu, S.; Zhu, Y.; Li, Y.; Dai, J.; Wang, C.; Liu, B.; Pastel, G.; Xie, H.; et al. Stabilizing the garnet solid-electrolyte/polysulfide interface in Li-S batteries. Chem. Mater. 2017, 29, 8037–8041.

55. Murugan, R.; Thangadurai, V.; Weppner, W. Fast lithium ion conduction in garnet-type Li7La3Zr2O12. Angew. Chem. In t. Ed. 2007, 46, 7778–7781.

56. Xiang, Y.X.; Zheng, G.; Zhong, G.; Wang, D.; Fu, R.; Yang, Y. Toward understanding of ion dynamics in highly conducti ve lithium ion conductors: Some perspectives by solid state NMR techniques. Solid State Ion. 2018, 318, 19–26.

57. Loho, C.; Djenadic, R.; Bruns, M.; Clemens, O.; Hahn, H. Garnet-type Li7La3Zr2O12 solid electrolyte thin films grown b y CO2-laser assisted CVD for all-solid-state batteries. J. Electrochem. Soc. 2016, 164, A6131–A6139.

58. Wang, Z.; Lee, J.Z.; Xin, H.L.; Han, L.; Grillon, N.; Guy-Bouyssou, D.; Bouyssou, E.; Proust, M.; Meng, Y.S. Effects of c athode electrolyte interfacial (CEI) layer on long term cycling of all-solid-state thin-film batteries. J. Power Sources 201 6, 324, 342–348.

59. Lobe, S.; Dellen, C.; Finsterbusch, M.; Gehrke, H.G.; Sebold, D.; Tsai, C.L.; Uhlenbruck, S.; Guillon, O. Radio frequenc y magnetron sputtering of Li7La3Zr2O12 thin films for solid-state batteries. J. Power Sources 2016, 307, 684–689.

60. Larfaillou, S.; Guy-Bouyssou, D.; le Cras, F.; Franger, S. Comprehensive characterization of all-solid-state thin films co mmercial microbatteries by electrochemical impedance spectroscopy. J. Power Sources 2016, 319, 139–146.

61. Yoon, M.; Lee, S.; Lee, D.; Kim, J.; Moon, J. All-solid-state thin film battery based on well-aligned slanted LiCoO2 nano wires fabricated by glancing angle deposition. Appl. Surf. Sci. 2017, 412, 537–544.

62. Wang, Y.; Roller, J.; Maric, R. Direct dry synthesis of thin nanostructured LiNi0.8Co0.2O2 film for lithium ion micro-batte ry cathodes. Electrochim. Acta 2017, 241, 510–516.

63. Larcher, D.; Tarascon, J.M. Towards greener and more sustainable batteries for electrical energy storage. Nat. Chem. 2 015, 7, 19–29.

64. Hagman, L.O.; Kierkegaard, P.; Karvonen, P. The crystal structure of NaMe2IV(PO4)3; MeIV = Ge, Ti, Zr. Acta Chem. S cand. 1968, 22, 1822–1832.

65. Anantharamulu, N.; Koteswara Rao, K.; Rambabu, G.; Vijaya Kumar, B.; Radha, V.; Vithal, M. A wide-ranging review on NASICON type materials. J. Mater. Sci. 2011, 46, 2821–2837.

66. Arbi, K.; Bucheli, W.; Jiménez, R.; Sanz, J. High lithium ion conducting solid electrolytes based on NASICON Li1+xAlx M2−x(PO4)3 materials (M = Ti, Ge and 0 ≤ x ≤ 0.5). J. Eur. Ceram. Soc. 2015, 35, 1477–1484.

67. Thokchom, J.S.; Kumar, B. The effects of crystallization parameters on the ionic conductivity of a lithium aluminum ger manium phosphate glass–ceramic. J. Power Sources 2010, 195, 2870–2876.

68. Safanama, D.; Adams, S. High efficiency aqueous and hybrid lithium-air batteries enabled by Li1.5Al0.5Ge1.5(PO4)3 c eramic anode-protecting membranes. J. Power Sources 2017, 340, 294–301.

69. Liu, Y.; Li, C.; Li, B.; Song, H.; Cheng, Z.; Chen, M.; He, P.; Zhou, H. Germanium thin film protected lithium aluminum g ermanium phosphate for solid-state Li batteries. Adv. Energy Mater. 2018, 8, 1702374.

70. Hong, H.P. Crystal structure and ionic conductivity of Li14Zn(GeO4)4 and other new Li+ superionic conductors. Mater. Res. Bull. 1978, 13, 117–124.

71. Knauth, P. Inorganic solid Li ion conductors: An overview. Solid State Ion. 2009, 180, 911–916

72. Kuwano, J.; West, A.R. New Li+ ion conductors in the system, Li4GeO4-Li3VO4. Mater. Res. Bull. 1980, 15, 1661–166 7.

73. Song, S.; Lu, J.; Zheng, F.; Duong, H.M.; Lu, L. A facile strategy to achieve high conduction and excellent chemical sta bility of lithium solid electrolytes. RSC Adv. 2015, 5, 6588–6594.

74. Kanno, R.; Murayama, M. Lithium ionic conductor thio-LISICON: The Li2S-GeS2-P2S5 system. J. Electrochem. Soc. 2 001, 148, A742–A746.

75. Bates, J.; Dudney, N.; Gruzalski, G.; Zuhr, R.; Choudhury, A.; Luck, C.; Robertson, J. Electrical properties of amorphou s lithium electrolyte thin films. Solid State Ion. 1992, 53, 647–654.

76. Fleutot, B.; Pecquenard, B.; Martinez, H.; Letellier, M.; Levasseur, A. Investigation of the local structure of LiPON thin fil ms to better understand the role of nitrogen on their performance. Solid State Ion. 2011, 186, 29–36.

77. Su, Y.; Falgenhauer, J.; Polity, A.; Leichtweiß, T.; Kronenberger, A.; Obel, J.; Zhou, S.; Schlettwein, D.; Janek, J.; Meye r, B.K. LiPON thin films with high nitrogen content for application in lithium batteries and electrochromic devices prepar ed by RF magnetron sputtering. Solid State Ion. 2015, 282, 63–69.

78. Tintignac, S.; Baddour-Hadjean, R.; Pereira-Ramos, J.P.; Salot, R. High rate bias sputtered LiCoO2 thin films as positiv e electrode for all-solid-state lithium microbatteries. Electrochim. Acta 2014, 146, 472–476.

79. Eftekhari, A. Fabrication of 5 V lithium rechargeable micro-battery. J. Power Sources 2004, 132, 240–243.

80. Lethien, C.; Zegaoui, M.; Roussel, P.; Tilmant, P.; Rolland, N.; Rolland, P.A. Micro-patterning of LiPON and lithium iron phosphate material deposited onto silicon nanopillars array for lithium ion solid state 3D micro-battery. Microelectron. E ng. 2011, 88, 3172–3177.

81. Inaguma, Y.; Liquan, C.; Itoh, M.; Nakamura, T.; Uchida, T.; Ikuta, H.; Wakihara, M. High ionic conductivity in lithium lant hanum titanate. Solid State Commun. 1993, 86, 689–693.

82. Alonso, J.A.; Sanz, J.; Santamaría, J.; León, C.; Várez, A.; Fernández-Díaz, M.T. On the location of Li+ cations in the fa st Li-cation conductor La0.5Li0.5TiO3 perovskite. Angew. Chem. Int. Ed. 2000, 39, 619–621.

83. Jay, E.E.; Rushton, M.J.; Chroneos, A.; Grimes, R.W.; Kilner, J.A. Genetics of superionic conductivity in lithium lanthan um titanates. Phys. Chem. Chem. Phys. 2015, 17, 178–183.

84. Lu, J.; Li, Y.; Ding, Y. Structure, stability, and ionic conductivity of perovskite Li2x-ySr1-x-yLayTiO3 solid electrolytes. Ce ram. Int. 2020, 46, 7741–7747.

85. Bohnke, O. Mechanism of ionic conduction and electrochemical intercalation of lithium into the perovskite lanthanum lit hium titanate. Solid State Ion. 1996, 91, 21–31.

86. Birke, P. Electrolytic stability limit and rapid lithium insertion in the fast-ion-conducting Li0.29La0.57TiO3 perovskite-typ e compound. J. Electrochem. Soc. 1997, 144, L167–L169.

87. Chen, C. Ionic conductivity, lithium insertion and extraction of lanthanum lithium titanate. Solid State Ion. 2001, 144, 51 –57.

88. Hu, Z.; Sheng, J.; Chen, J.; Sheng, G.; Li, Y.; Fu, X.Z.; Wang, L.; Sun, R.; Wong, C.P. Enhanced Li ion conductivity in G e-doped Li0.33La0.56TiO3 perovskite solid electrolytes for all-solid-state Li-ion batteries. New J. Chem. 2018, 42, 9074 –9079.

89. Chen, C. Stable lithium-ion conducting perovskite lithium-strontium-tantalum-zirconium-oxide system. Solid State Ion. 2 004, 167, 263–272.

90. Luntz, A.C.; Voss, J.; Reuter, K. Interfacial challenges in solid-state Li ion batteries. J. Phys. Chem. Lett. 2015, 6, 4599–4604.

91. Takada, K.; Ohta, N.; Zhang, L.; Fukuda, K.; Sakaguchi, I.; Ma, R.; Osada, M.; Sasaki, T. Interfacial modification for high-power solid-state lithium batteries. Solid State Ion. 2008, 179, 1333–1337.

92. Hartmann, P.; Leichtweiss, T.; Busche, M.R.; Schneider, M.; Reich, M.; Sann, J.; Adelhelm, P.; Janek, J. Degradation of NASICON-type materials in contact with lithium metal: Formation of mixed conducting interphases (MCI) on solid electrolytes. J. Phys. Chem. C. 2013, 117, 21064–21074.

93. Pan, Q.; Barbash, D.; Smith, D.M.; Qi, H.; Gleeson, S.E.; Li, C.Y. Correlating electrode-electrolyte interface and battery performance in hybrid solid polymer electrolyte-based lithium metal batteries. Adv. Energy Mater. 2017, 7, 1701231.

94. Wu, B.; Wang, S.; Evans Iv, W.J.; Deng, D.Z.; Yang, J.; Xiao, J. Interfacial behaviours between lithium ion conductors and electrode materials in various battery systems. J. Mater. Chem. A 2016, 4, 15266–15280.

95. Kitaura, H.; Hayashi, A.; Ohtomo, T.; Hama, S.; Tatsumisago, M. Fabrication of electrode-electrolyte interfaces in all-solid-state rechargeable lithium batteries by using a supercooled liquid state of the glassy electrolytes. J. Mater. Chem. 2011, 21, 118–124.

96. Ohta, S.; Seki, J.; Yagi, Y.; Kihira, Y.; Tani, T.; Asaoka, T. Co-sinterable lithium garnet-type oxide electrolyte with cathode for all-solid-state lithium ion battery. J. Power Sources 2014, 265, 40–44.

97. Koerver, R.; Zhang, W.; de Biasi, L.; Schweidler, S.; Kondrakov, A.O.; Kolling, S.; Brezesinski, T.; Hartmann, P.; Zeier, W.G.; Janek, J. Chemo-mechanical expansion of lithium electrode materials–on the route to mechanically optimized all-solid-state batteries. Energy Environ. Sci. 2018, 11, 2142–2158.

98. Koerver, R.; Aygün, I.; Leichtweiß, T.; Dietrich, C.; Zhang, W.; Binder, J.O.; Hartmann, P.; Zeier, W.G.; Janek, J. Capacity fade in solid-state batteries: Interphase formation and chemomechanical processes in nickel-rich layered oxide cathodes and ithium thiophosphate solid electrolytes. Chem. Mater. 2017, 29, 5574–5582.

99. Bucci, G.; Talamini, B.; Renuka Balakrishna, A.; Chiang, Y.M.; Carter, W.C. Mechanical instability of electrode-electrolyte interfaces in solid-state batteries. Phys. Rev. Mater. 2018, 2, 105407.

100. Zhang, W.; Schröder, D.; Arlt, T.; Manke, I.; Koerver, R.; Pinedo, R.; Weber, D.A.; Sann, J.; Zeier, W.G.; Janek, J. (Electro) chemical expansion during cycling: Monitoring the pressure changes in operating solid-state lithium batteries. J. Mater. Chem. A 2017, 5, 9929–9936.

101. Sakuda, A.; Kitaura, H.; Hayashi, A.; Tadanaga, K.; Tatsumisago, M. Improvement of high-rate performance of all-solid-state lithium secondary batteries using LiCoO2 coated with Li2O-SiO2 glasses. Electrochem. Solid-State Lett. 2008, 11, A1.

102. Ohta, S.; Komagata, S.; Seki, J.; Saeki, T.; Morishita, S.; Asaoka, T. All-solid-state lithium ion battery using garnet-type oxide and Li3BO3 solid electrolytes fabricated by screen-printing. J. Power Sources 2013, 238, 53–56.

103. Zhang, W.; Richter, F.H.; Culver, S.P.; Leichtweiss, T.; Lozano, J.G.; Dietrich, C.; Bruce, P.G.; Zeier, W.G.; Janek, J. Degradation mechanisms at the Li10GeP2S12/LiCoO2 cathode interface in an all-solid-state lithium-ion battery. ACS Appl. Mater. Interfaces 2018, 10, 22226–22236.

104. Morimoto, H.; Awano, H.; Terashima, J.; Shindo, Y.; Nakanishi, S.; Ito, N.; Ishikawa, K.; Tobishima, S.I. Preparation of lithium ion conducting solid electrolyte of NASICON-type Li1+xAlxTi2−x(PO4)3 (x = 0.3) obtained by using the mechanochemical method and its application as surface modification materials of LiCoO2 cathode for lithium cell. J. Power Sources 2013, 240, 636–643.

105. Richards, W.D.; Miara, L.J.; Wang, Y.; Kim, J.C.; Ceder, G. Interface stability in solid-state batteries. Chem. Mater. 2016, 28, 266–273.

106. Takada, K.; Ohta, N.; Tateyama, Y. Recent Progress in interfacial nanoarchitectonics in solid-state batteries. J. Inorg. Organomet. Polym. Mater. 2015, 25, 205–213.

107. Miara, L.; Windmüller, A.; Tsai, C.L.; Richards, W.D.; Ma, Q.; Uhlenbruck, S.; Guillon, O.; Ceder, G. About the compatibility between high voltage spinel cathode materials and solid oxide electrolytes as a function of temperature. ACS Appl. Mater. Interfaces 2016, 8, 26842–26850.

108. Yamamoto, K.; Iriyama, Y.; Asaka, T.; Hirayama, T.; Fujita, H.; Fisher, C.A.J.; Nonaka, K.; Sugita, Y.; Ogumi, Z. Dynamic visualization of the electric potential in an all-solid-state rechargeable lithium battery. Angew. Chem. 2010, 49, 4414–4417.

109. Masuda, H.; Ishida, N.; Ogata, Y.; Ito, D.; Fujita, D. Internal potential mapping of charged solid-state-lithium ion batteries using in situ Kelvin probe force microscopy. Nanoscale 2017, 9, 893–898.

110. Haruta, M.; Shiraki, S.; Suzuki, T.; Kumatani, A.; Ohsawa, T.; Takagi, Y.; Shimizu, R.; Hitosugi, T. Negligible “negative space-charge layer effects” at oxide-electrolyte/electrode interfaces of thin-film batteries. Nano Lett. 2015, 15, 1498–1502.

111. de Klerk, N.J.J.; Wagemaker, M. Space-charge layers in all-solid-state batteries; important or negligible? ACS Appl. Energy Mater. 2018, 1, 5609–5618.

112. Okumura, T.; Nakatsutsumi, T.; Ina, T.; Orikasa, Y.; Arai, H.; Fukutsuka, T.; Iriyama, Y.; Uruga, T.; Tanida, H.; Uchimoto, Y.; et al. Depth-resolved X-ray absorption spectroscopic study on nanoscale observation of the electrode-solid electrolyte interface for all solid state lithium ion batteries. J. Mater. Chem. 2011, 21, 10051–10060.

113. Wenzel, S.; Leichtweiss, T.; Krüger, D.; Sann, J.; Janek, J. Interphase formation on lithium solid electrolytes–an in situ approach to study interfacial reactions by photoelectron spectroscopy. Solid State Ion. 2015, 278, 98–105.

114. Bron, P.; Roling, B.; Dehnen, S. Impedance characterization reveals mixed conducting interphases between sulfidic superionic conductors and lithium metal electrodes. J. Power Sources 2017, 352, 127–134.

115. Mizuno, F.; Yada, C.; Iba, H. Solid-state lithium-ion batteries for electric vehicles. In Lithium-Ion Batteries, 1st ed.; Pistoia, G., Ed.; Elsevier: Amsterdam, The Netherlands, 2014; pp. 273–291.

116. Park, K.; Yu, B.C.; Jung, J.W.; Li, Y.; Zhou, W.; Gao, H.; Son, S.; Goodenough, J.B. Electrochemical nature of the cathode interface for a solid-state lithium-ion battery: Interface between LiCoO2 and garnet-Li7La3Zr2O12. Chem. Mater. 2016, 28, 8051–8059.

117. Wenzel, S.; Randau, S.; Leichtweiß, T.; Weber, D.A.; Sann, J.; Zeier, W.G.; Janek, J. Direct observation of the interfacial instability of the fast ionic conductor Li10GeP2S12 at the lithium metal anode. Chem. Mater. 2016, 28, 2400–2407.

118. Han, X.; Gong, Y.; Fu, K.; He, X.; Hitz, G.T.; Dai, J.; Pearse, A.; Liu, B.; Wang, H.; Rubloff, G.; et al. Negating interfacial impedance in garnet-based solid-state Li metal batteries. Nat. Mater. 2017, 16, 572–579.

119. Ohta, N.; Takada, K.; Zhang, L.; Ma, R.; Osada, M.; Sasaki, T. Enhancement of the high-rate capability of solid-state lithium batteries by nanoscale interfacial modification. Adv. Mater. 2006, 18, 2226–2229.

120. Dudney, N.; Neudecker, B. Solid state thin-film lithium battery systems. Curr. Opin. Solid State Mater. Sci. 1999, 4, 479–482.

121. Wang, Y.; Liu, B.; Li, Q.; Cartmell, S.; Ferrara, S.; Deng, Z.D.; Xiao, J. Lithium and lithium ion batteries for applications in microelectronic devices: A review. J. Power Sources 2015, 286, 330–345.

122. Oudenhoven, J.F.; Baggetto, L.; Notten, P.H. All-solid-state lithium-ion microbatteries: A review of various three-dimensional concepts. Adv. Energy Mater. 2011, 1, 10–33.

123. Kanehori, K.; Matsumoto, K.; Miyauchi, K.; Kudo, T. Thin film solid electrolyte and its application to secondary lithium cell. Solid State Ion. 1983, 9, 1445–1448.

124. Ohtsuka, H.; Yamaki, J.I. Electrical characteristics of Li2O-V2O5-SiO2 thin films. Solid State Ion. 1989, 35, 201–206.

125. Jourdaine, L.; Souquet, J.; Delord, V.; Ribes, M. Lithium solid state glass-based microgenerators. Solid State Ion. 1988, 28, 1490–1494.

126. Balkanski, M.; Julien, C.; Emery, J. Integrable lithium solid-state microbatteries. J. Power Sources 1989, 26, 615–622.

127. Bates, J.; Gruzalski, G.; Dudney, N.; Luck, C.; Yu, X. Rechargeable thin-film lithium batteries. Solid State Ion. 1994, 70, 619–628.

128. Long, J.W.; Dunn, B.; Rolison, D.R.; White, H.S. Three-dimensional battery architectures. Chem. Rev. 2004, 104, 4463–4492.

129. Garbayo, I.; Struzik, M.; Bowman, W.J.; Pfenninger, R.; Stilp, E.; Rupp, J.L. Glass-Type polyamorphism in Li-garnet thin film solid state battery conductors. Adv. Energy Mater. 2018, 8, 1702265

130. Ferrari, S.; Loveridge, M.; Beattie, S.D.; Jahn, M.; Dashwood, R.J.; Bhagat, R. Latest advances in the manufacturing of 3D rechargeable lithium microbatteries. J. Power Sources 2015, 286, 25–46.

131. Julien, C.M.; Mauger, A. Pulsed laser deposited films for microbatteries. Coatings 2019, 9, 386.

132. Dudney, N.J. Solid-state thin-film rechargeable batteries. Mater. Sci. Eng.: B 2005, 116, 245–249.

133. Bates, J.; Gruzalski, G.; Dudney, N.; Luck, C.; Yu, X.; Jones, S. Rechargeable thin-film lithium microbatteries. Solid State Technol. 1993, 36, 59–64.

134. Jones, S.D.; Akridge, J.R. A thin film solid state microbattery. Solid State Ion. 1992, 53, 628–634.

135. Lee, S.J.; Baik, H.K.; Lee, S.M. An all-solid-state thin film battery using LISIPON electrolyte and Si-V negative electrode films. Electrochem. Commun. 2003, 5, 32–35.

136. Zhou, Y.N.; Xue, M.Z.; Fu, Z.W. Nanostructured thin film electrodes for lithium storage and all-solid-state thin-film lithium batteries. J. Power Sources 2013, 234, 310–332.
137. Patil, A.; Patil, V.; Shin, D.W.; Choi, J.W.; Paik, D.S.; Yoon, S.J. Issue and challenges facing rechargeable thin film lithium batteries. Mater. Res. Bull. 2008, 43, 1913–1942.
138. Randau, S.; Weber, D.A.; Kötz, O.; Koerver, R.; Braun, P.; Weber, A.; Ivers-Tiffée, E.; Adermann, T.; Kulisch, J.; Zeier, W.G.; et al. Benchmarking the performance of all-solid-state lithium batteries. Nat. Energy 2020, 5, 259–270.
139. Tarascon, J.M.; Armand, M. Issues and challenges facing rechargeable lithium batteries. In Materials for Sustainable Energy; Dusastre, V., Ed.; World Scientific: Singapore, 2010; pp. 171–179.
140. Zhang, W.; Liu, Y.; Guo, Z. Approaching high-performance potassium-ion batteries via advanced design strategies and engineering. Sci. Adv. 2019, 5, eaav7412.
141. Hwang, H.Y.; Iwasa, Y.; Kawasaki, M.; Keimer, B.; Nagaosa, N.; Tokura, Y. Emergent phenomena at oxide interfaces Nat. Mater. 2012, 11, 103–113.
142. Zubko, P.; Gariglio, S.; Gabay, M.; Ghosez, P.; Triscone, J.M. Interface physics in complex oxide heterostructures. Annu. Rev. Condens. Matter Phys. 2011, 2, 141–165.
143. Brinkman, A.; Huijben, M.; van Zalk, M.; Huijben, J.; Zeitler, U.; Maan, J.C.; van der Wiel, W.G.; Rijnders, G.; Blank, D.H.A.; Hilgenkamp, H. Magnetic effects at the interface between non-magnetic oxides. Nat. Mater. 2007, 6, 493–496.
144. Ohtomo, A.; Hwang, H.Y. A high-mobility electron gas at the LaAlO3/SrTiO3 heterointerface. Nature 2004, 427, 423–426.
145. Pomerantseva, E.; Gogotsi, Y. Two-dimensional heterostructures for energy storage. Nat. Energy 2017, 2, 17089.
146. Suzuki, K.; Kim, K.; Taminato, S.; Hirayama, M.; Kanno, R. Fabrication and electrochemical properties of LiMn2O4/SrRuO3 multi-layer epitaxial thin film electrodes. J. Power Sources 2013, 226, 340–345.
147. Aierken, Y.; Sevik, C.; Gülseren, O.; Peeters, F.M.; Çakır, D. MXenes/graphene heterostructures for Li battery applications: A first principles study. J. Mater. Chem. A 2018, 6, 2337–2345.
148. Chueh, W.C.; Hao, Y.; Jung, W.; Haile, S.M. High electrochemical activity of the oxide phase in model ceria-Pt and ceria-Ni composite anodes. Nat. Mater. 2012, 11, 155–161.
149. Lee, D.; Gao, X.; Sun, L.; Jee, Y.; Poplawsky, J.; Farmer, T.O.; Fan, L.; Guo, E.J.; Lu, Q.; Heller, W.T.; et al. Colossal oxygen vacancy formation at a fluorite-bixbyite interface. Nat. Commun. 2020, 11, 1371.
150. Yang, Y.; Peng, Z.; Wang, G.; Ruan, G.; Fan, X.; Li, L.; Fei, H.; Hauge, R.H.; Tour, J.M. Three-dimensional thin film for lithium-ion batteries and supercapacitors. ACS Nano 2014, 8, 7279–7287.
151. Choi, B.G.; Chang, S.J.; Lee, Y.B.; Bae, J.S.; Kim, H.J.; Huh, Y.S. 3D heterostructured architectures of Co3O4 nanoparticles deposited on porous graphene surfaces for high performance of lithium ion batteries. Nanoscale 2012, 4, 5924–5930.